

A SEARCH FOR SOLAR-LIKE OSCILLATIONS IN ALPHA CENTAURI A

TIMOTHY M. BROWN AND RONALD L. GILLILAND

High Altitude Observatory/National Center for Atmospheric Research¹

Received 1988 November 28; accepted 1989 August 22

ABSTRACT

We describe spectrographic observations made in the course of a search for solar-like acoustic oscillations in α Cen A. The observational method was to search for periodic Doppler-shift variations in all of the spectrum lines within the wavelength range accessible to a high-dispersion echelle spectrograph—about 30 nm centered on 427.5 nm, in our case. We also searched for variations in the ratio of line core to continuum intensity, again averaged over all the available lines. We found no convincing oscillations in either case, with upper limits for typical single oscillation modes of 70 cm s^{-1} in Doppler shift and 4×10^{-5} for continuum intensity variations inferred from line core intensities.

Subject headings: stars: individual (α Cen) — stars: pulsation — Sun: oscillations

I. INTRODUCTION

Solar p -mode oscillations have become a fruitful source of information about solar structure (see, e.g., Brown and Morrow 1987). Motivated by the solar example, several recent attempts have been made to detect solar-like oscillations on other stars, though none of these has succeeded unambiguously. Noyes *et al.* (1984) may have seen oscillations in the Ca II intensity of ϵ Eri, but only on some nights, and with amplitude ~ 100 times that expected. Gelly, Grec, and Fossat (1986, 1988) report detection of velocity oscillations on Procyon with periods of 10–25 minutes, although more recent observations (B. Gelly, private communication, 1988) suggest that this detection may have been spurious. Fossat, Gelly, and Grec (1984) and Gelly, Grec, and Fossat (1986) report detections on α Cen A, using a sodium resonance cell to measure Doppler shifts. However, the separation between oscillation frequencies derived from the α Cen observations is inconsistent with our current knowledge of that star. It is thus a matter of great current interest to obtain an *unambiguous* detection of oscillations on stars of near-solar type.

The solar p -modes are distinguished by their short periods (5 minutes), their large radial order (typically 20, for large spatial scales) and their small amplitudes (20 cm s^{-1} in velocity for single modes, or 3×10^{-6} in relative continuum intensity). Although many inferences about the solar interior rely on observation of strongly nonradial oscillations, there is much to learn from oscillations with angular degree l between 0–3. This range of l may be detected using disk-integrated light, and hence is accessible even on distant stars. The frequency spectrum for such oscillations consists of pairs of modes with $l = 0, 2$ and $l = 1, 3$. The modes in each pair have nearly identical frequencies, and the pairs are separated by $\nu_0/2$, where ν_0 is a parameter determined principally by the star's radius. Conditions in the stellar core determine the splitting between modes within each pair. For the Sun, ν_0 is $\sim 136 \mu\text{Hz}$; ν_0 decreases as the stellar radius increases. To learn anything about the star, one must observe its variations for 8–12 hours—long enough to resolve this frequency difference. Measuring ν_0 would provide an accurate measure of the stellar radius. The splitting between modes with $l = 0$ and $l = 2$ is typically 8–12 μHz in

cool dwarfs; it is expected to decrease as the star evolves. An observed value for the splitting would allow an estimate of the star's evolutionary state (see, e.g., Christensen-Dalsgaard 1988). Observation of this splitting in the Sun suggests that lower sound speeds exist in the solar core than is expected from standard models. This discrepancy would be explained by lower effective core opacities, and thus lower temperatures; a result which would also be consistent with the well known deficit of predicted solar neutrinos (see, e.g., Gilliland and Däppen 1988).

A complication arises when one contemplates a careful analysis of the frequency splittings of stellar oscillations. This is that for all stars except the Sun, fundamental stellar parameters (like the age, mass, and composition) are ordinarily quite poorly known. Unobservably small variations in metallicity are particularly likely to confuse interpretation of frequency splitting data, were such available (Gough 1987). The value of oscillations data thus increases dramatically if other precise information is available about the star in question. For this reason, well-observed visual binaries are particularly interesting; such stars may be assumed nearly coeval, with similar initial compositions, and moreover are likely to have well-determined mass ratios and possibly parallaxes.

Since solar-like oscillations in other stars have not yet been seen, one must also be concerned with questions of existence and detectability. The source of excitation for the solar oscillations is not known with certainty, so one is not sure where in the H-R diagram to search for stars that might behave similarly to the Sun. About all that can be said is that solar-like stars should probably be oscillating with solar-like amplitudes. One is thus motivated to start with stars of near-solar type, and move out in the H-R diagram as our knowledge of the oscillation process improves. Since the expected amplitudes are so small, one is also driven to observe bright stars. With the telescopes that are currently available and optimal detection schemes, photon statistics set detectability limits that are not much smaller than the expected amplitudes, even for the brightest stars in the sky (Connes 1985). If technical limits force one to suboptimal detection methods (as always happens), matters are that much worse.

In view of these considerations, the α Cen system occupies a unique place as an observable, understandable object. Alpha Cen is a well-observed visual binary, with an orbital period of

¹ The National Center for Atmospheric Research is sponsored by the National Science Foundation.

about 80 yr and maximum separation of $\sim 20''$. Both of its bright components are of near-solar type, and in fact they straddle the Sun in mass, surface temperature, and luminosity. Finally, they are bright ($m_v = 0.1, 1.4$), and at the appropriate time of year are well placed for long uninterrupted periods of observation. Observed properties and theoretical modeling of the α Cen system are described in detail by Flannery and Ayres (1978).

II. OBSERVATIONS

We observed α Cen A using the CTIO 1.5 m telescope for a total of ~ 29 hours during the nights of 1987 May 11–15. During much of this time the sky was partly cloudy. On our best single night (May 14–15), we were able to observe for 10 hours almost continuously. Starlight arriving at the focus of the 1.5 m telescope was carried through an optical fiber for a distance of some 50 m to the CTIO 4 m echelle spectrograph, which was stationary on the floor of the 4 m dome. The fiber used had a diameter of $150 \mu\text{m}$, which projected onto $2.7''$ in the sky. The echelle spectrograph setup allowed us to observe $\sim 99\%$ of the wavelength region between 412 and 443 nm in nine consecutive echelle orders. Using the RCA No. 5 detector we were able to obtain resolution of $\sim 34,000$ (2 pixel), corresponding to a Doppler scale of $\sim 4400 \text{ m s}^{-1} \text{ pixel}^{-1}$.

We took sequences of 60 s exposures, which with detector readout time and other overhead yielded a mildly irregular interval between exposures, averaging ~ 83 s. The actual observing intervals and number of images collected are described in Table 1. With the star image properly centered on the optical fiber, a 60 s exposure gave $\sim 10^5$ photoelectrons per pixel in the continuum near the center of our wavelength range, corresponding to a maximum signal-to-noise (S/N) ratio of ~ 300 . In order to attain this low noise level, it was necessary to calibrate the CCD response rather carefully. For this purpose we took several kinds of calibration exposures at the beginning, end, and sometimes in the middle of each night. In addition to the usual bias and dark exposures, we took flat field exposures generated with a quartz lamp shining through the fiber from the telescope end. Because instabilities in the spectrograph and dewar caused small motions of the spectrum both parallel and perpendicular to the dispersion, it would have been better to perform flat fields with an effective slit significantly longer than that provided by the fiber. This was not possible, but it probably makes little difference in our results. We investigated the low-level nonlinear (deferred charge) behavior of the CCD by performing a series of graded preflash exposures. These revealed that, at least for some pixels, deferred charge corrections may be important for the RCA No. 5 chip. Finally, in order to establish an accurate wavelength scale and to estimate the intrinsic mechanical and thermal stability of the spectrograph, we performed several time series observations of a thorium-argon lamp. The light from this lamp also reached the spectrograph through the fiber.

III. DATA REDUCTION

We applied a number of corrections to the raw data before attempting to extract spectra. These were corrections for overscan, bias, dark current, and deferred charge. The first two of these correct for small, possibly time-varying offsets in the chip and readout electronics—ones that may be sampled in a CCD exposure of zero duration. The dark current correction compensates for the spatially variable leakage current that builds

TABLE 1
LOG OF OBSERVATIONS

Date	UT Interval	Number of Images
1987 May 12	0:49–2:07	76
1987 May 13	6:13–9:27	124
1987 May 14	1:14–9:19	325
1987 May 14–15	23:30–9:30	407
1987 May 16	0:53–7:19	170

up on the chip during a finite exposure, even when it is not exposed to light. The deferred charge correction accounts for nonlinear behavior of the chip at low light levels, modeled as a spatially dependent amount of charge that must accumulate on each pixel before its output rises above zero. These corrections are discussed in detail in, for example, Gilliland and Brown (1988).

Had long-slit field exposures been available, we would have used them to correct for spatial gain variations at this point in the reductions. Since they were not, we proceeded with extraction of one-dimensional spectra. We tried several methods with various levels of sophistication for extracting spectra from the images. The simplest technique was to perform an unweighted sum of the measured intensities in the direction perpendicular to the dispersion. The most complex of the methods involved determining the shape of the intensity distribution perpendicular to the dispersion (the *point-spread function* [PSF]), and at each point along the dispersion doing a weighted least-squares fit to the measured intensities, with a factor multiplying this PSF as a parameter (see, e.g., Horne 1986). This multiplier is then taken to be the intensity at each wavelength. With our low noise spectra it developed that the differences between results from these methods were quite small.

This extraction yielded intensity as a function of distance along the order of each of the nine complete echelle orders, for each image. We corrected these spectra for spatial variations in the chip gain by dividing them point-by-point by similar spectra of the quartz-iodine continuum source. This was not the ideal way to perform this correction, since chip motion and other spectrograph drifts generally caused the stellar and continuum spectra to sample slightly different parts of the chip. It was, however, the best that could be done, lacking long-slit flat field exposures. In addition to the intensity values, we computed several other numbers relating to each order taken as a unit. These were derived by fitting Gaussians to the measured intensities averaged parallel to the dispersion, for each order. These fits yielded values for the mean width, amplitude, and position (perpendicular to the dispersion) of each order.

An important and useful property of echelle spectra is that in the spectrograph image plane, $1/\lambda d\lambda/dx$ is very nearly a constant, independent of order or of position within orders. As a result, Doppler shifts appear as translations of the entire spectrum in the direction parallel to the dispersion, with no stretching or deformation of the spectra. This property considerably simplifies the determination of Doppler shifts. It also implies, of course, that chip motion and most other spectrograph alignment instabilities have a form that is indistinguishable from that of a Doppler shift. One is therefore dependent on the mechanical and thermal stability of the spectrograph, at least for times comparable to the oscillation period of the star under observation.

To estimate shifts of the spectrum relative to the chip

(henceforth referred to as the Doppler signal), we used two methods. Both methods started by preflattening the spectra, which we did by dividing them by their convolution with a broad Gaussian. We next determined a grand average spectrum by averaging all of the spectra for a given night. In the simpler technique, we cross-correlated this average spectrum with each of the individual ones, adopting the lag at which this correlation reached its maximum as the offset between the current image and the average one. Since this lag was never very far from zero, we could estimate its position efficiently by computing the cross correlation for three points suitably spaced about zero lag, and then using parabolic interpolation to find the maximum. The other method we used was to shift the average spectrum with a suitable interpolation technique (we found Fourier interpolation to be the best in our case), and choose as the Doppler signal that shift which minimized the weighted mean-squared difference between the shifted scaled average spectrum and the image being considered. This method, though better in principle than the cross-correlation, was worse in practice. It gave noise levels that were typically 10% higher than those from the cross-correlation method, suggesting that noise was being introduced in the interpolation process. Since our data were at best marginally sampled in the dispersion direction, this result is perhaps not surprising.

In addition to time series of the Doppler signal, we computed another quantity that was intended to measure changes in the intensities of line cores relative to the continuum. This procedure was motivated by observations by Holweger and Testerman (1975) and by Harvey (1988), and theoretical work by Frandsen (1984), showing that p -modes in a stellar atmosphere cause intensity variations within line cores that are much larger (relative to their mean values) than are the continuum variations. By measuring line depths, one therefore obtains a quantity that is sensitive to stellar oscillations, but that is not affected by changing atmospheric transparency, scintillation, or motion of the spectrum relative to the chip (although one is still sensitive to spectrograph instabilities that change the point spread function). To perform this measurement in an optimal way, we first required a model of the oscillating intensity. For simplicity we modeled this as a linear function of intensity (referred to the local continuum):

$$\delta I_j = A I_{cj} \left(1 - k \frac{I_j - I_{cj}}{I_{cj}} \right), \quad (1)$$

where δI_j is the oscillating signal at wavelength λ_j , and I_j and I_{cj} are the observed and continuum intensities for that wavelength, as estimated from the mean spectrum. In equation (1), A is the oscillating amplitude (expected to be a few times 10^{-6} for solar-like oscillations). The parameter k in equation (1) relates the oscillating variation in continuum intensity to that in the line core. When $k = 0$, oscillations cause the intensity to change by the same absolute amount everywhere in the line profile (causing the relative intensity variation to be largest in the line core). For $k > 0$ line core variations are larger than those in the continuum in absolute terms. Ideally, k would be determined by using a radiative transfer model to calculate the changes in the shape of spectrum lines resulting from the presence of stellar oscillations. In practice, one has little information about k except for the observations by Holweger and Testerman (1975) and the calculations by Frandsen (1984). For our purposes we tried several values of k , ranging between 0–5. Given this model, the observed mean spectrum, and some

knowledge about the detection process, we could then compute for each pixel the expected signal δI_j and the expected rms noise N_j . N_j was determined from the (presumed independent) contributions of shot noise, dark current noise, and detector readout noise. From these functions of wavelength, we wished to produce a single number related to the line strength variations, with the best possible S/N ratio. To this end, we computed a set of weights W_j chosen to maximize

$$\frac{\sum_j W_j \delta I_j}{\left(\sum_j W_j^2 N_j^2 \right)^{1/2}}, \quad (2)$$

subject to

$$\sum_j W_j^2 = 1 \quad (3)$$

and

$$\sum_j W_j I_j = 0. \quad (4)$$

The desired oscillating line-depth signal was then $L(t) \equiv \sum_j W_j \delta I_j(t)$. Equation (3) is a normalization condition on the weights, while equation (4) assures that the weights are orthogonal to the mean spectrum, and hence that variations in the system transmission do not appear as additive noise in the output signal $L(t)$. Transmission variations may still appear as multiplicative noise, however, so it is useful to normalize all of the observed spectra (averaged over wavelength) to some standard intensity before computing $L(t)$.

The raw time series corresponding to the Doppler and line-depth signals consist of small variations superposed on variable trends with long time scales, and with occasional gaps and discontinuities (see Fig. 1). These trends were more apparent for the Doppler signal than for the line depth signal, which is not surprising in view of the intrinsically differential nature of the line depth measurement. Since we were only concerned with stellar oscillations with periods shorter than ~ 15 minutes, we were able to lower the detectable signal level by high-pass filtering the time series, and by removing correlations with known instrumental instabilities. The high-pass filter was implemented by convolving each timestring with a Gaussian with a FWHM of 500 s, and subtracting this smoothed time series from the original. All timestrings (including those measuring order width, height, and position) were high-pass filtered in this fashion. To further reduce the noise in the bandpass of interest, we then supposed that various instrumental instabilities might simultaneously affect the measurement of more than one of our observed quantities. For example, it is easy to imagine mechanisms whereby changing collimator illumination can cause changes in both the Doppler signal and the width of the spectrum orders. To investigate this possibility, we formed a correlation matrix, whose elements consisted of the cross-correlations of each possible pair of measured quantities. It developed that the mean intensity and the order width were significantly correlated with the Doppler signal. By subtracting appropriate multiples of the instrumental quantities from the Doppler signal, it was possible to remove this correlation and reduce the variance of the latter by $\sim 20\%$. For time series containing many independent observations, it is highly unlikely that this decorrelation process will remove a significant fraction of any true stellar signal. If the stellar and instrumental signals arise from independent random processes with N_j degrees of freedom, then one expects the power in the stellar signal to be reduced to

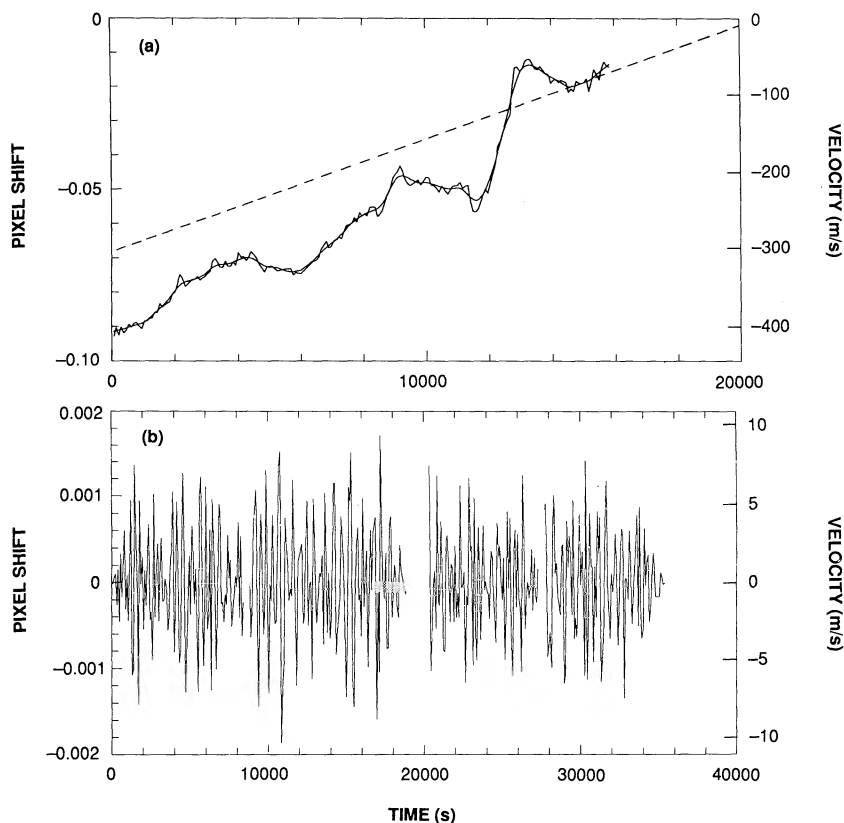


FIG. 1.—Doppler signal time series for the night of 1987 May 14–15. Panel (a) shows the raw Doppler signal for the first half of the night with a Gaussian-smoothed signal superposed, and a separate curve indicating the Doppler variation expected from the Earth's rotation. Panel (b) shows the residual (for the full night) after the smoothed signal is subtracted. The ordinates on the left-hand side are in units of CCD detector pixels, and on the right-hand side in m s^{-1} . Gaps in the data are shown as missing segments in panel (b), and in this panel, points that deviate from zero by more than 4σ have been excluded.

roughly $1 - N_f^{-1}$ of its true value. Note, however, that slow variations in stellar and instrumental parameters may be well correlated even though they arise from completely different processes, because in such cases the effective N_f is small. High-pass filtering both time series before cross-correlating is therefore essential. All of the time series that we shall discuss below were processed in this manner.

After this processing, the Doppler time series displayed typical rms values of $\sim 3.5 \text{ m s}^{-1}$, while that of the line depth signal (scaled to correspond to the continuum relative intensity fluctuation, assuming $k = 0$) was $\sim 10^{-4}$. Note that the scaling that should be applied to the latter quantity depends on the model used for intensity variations within the stellar absorption lines, and is therefore uncertain by perhaps a factor of 2.

IV. RESULTS

Figure 2 shows power spectra of the Doppler signal and line-depth signal, derived from time series spanning our four best nights. Since the measurements are unevenly spaced in time, we used the technique described by Scargle (1982) to compute the spectra. Both of these spectra may be characterized (at least approximately) as white noise, and there is no obvious indication in either one of the regular peak spacing that should characterize stellar p -modes. As indicated on the figures, the mean power levels correspond to amplitudes for single frequency bins of about ($\delta v = 35 \text{ cm s}^{-1}$ and $\delta I/I = 2 \times 10^{-5}$) for the Doppler and line depth signals, respec-

tively. The largest peaks in the spectra correspond to amplitudes of about $\delta v = 80 \text{ cm s}^{-1}$ and $\delta I/I = 4 \times 10^{-5}$.

Figure 3 shows one realization of a synthetic power spectrum in which a solar-like oscillation spectrum with the amplitude reported by Gelly, Grec, and Fossat 1986 has been added to white noise with the same amplitude as in Figure 2a. It is immediately clear from this figure that oscillations at the level reported by Gelly, Grec, and Fossat would have been detected, a conclusion that also follows from the Doppler rms of the high-passed time string shown in Figure 1b. A more important issue to settle is whether stellar oscillations are present at significantly lower amplitudes, that is, whether some of the peaks in the spectra shown in Figures 2a and 2b may be identified with stellar oscillation modes. We approach this question in two different ways: by examining the power spectra of the power spectra, and by investigating the statistics of the peak height distribution.

One may gain some sensitivity in detecting such a regular mode sequence by examining the power spectrum of the power spectrum (Gelly, Grec, and Fossat 1986). As we shall see, with noisy gapped data this procedure leads to conclusions that are less clear-cut than one might suppose, but it is nevertheless a useful one to follow. Figure 4 shows the power spectrum of the power spectrum of the Doppler signal, masked so that only frequencies between 1.5 and 3.5 mHz contribute to the result. The abscissa in this figure is period (in μHz) in the power spectrum. Simulations with scaled solar p -mode spectra indi-

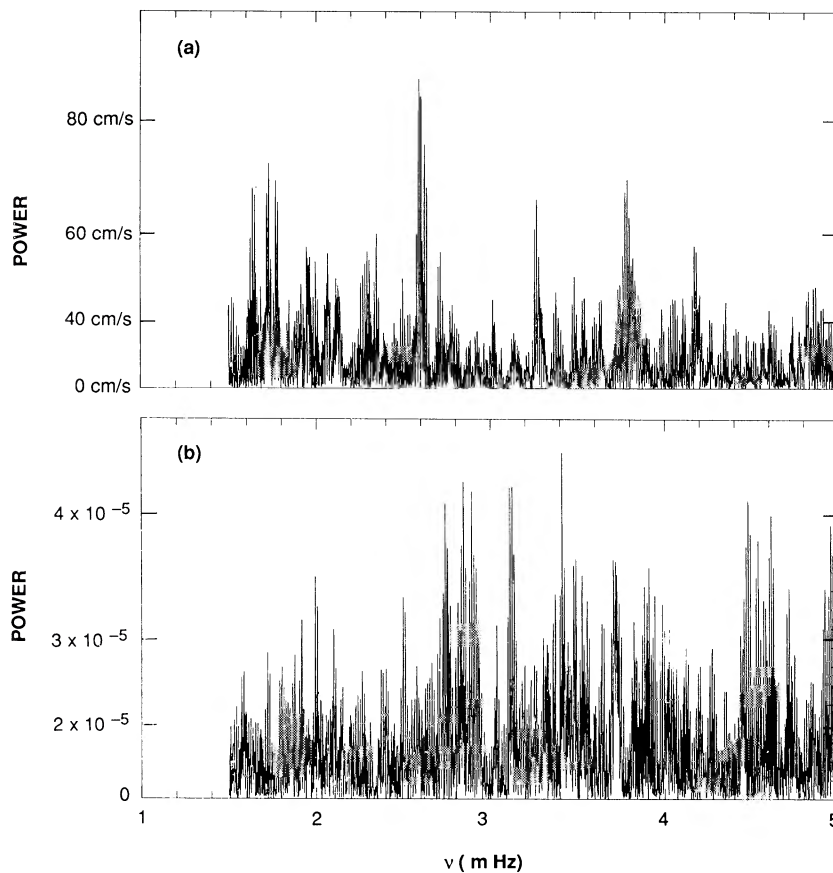


FIG. 2.—Power spectra of (a) Doppler signal and (b) line depth signal computed from the four-day sequence May 13–16. The frequency resolution in these spectra is $\sim 4 \mu\text{Hz}$. Frequencies below $\sim 1.5 \text{ mHz}$ are strongly attenuated by the high-pass filtering. The amplitude scales indicated on the figure are derived from passing sinusoids of known amplitude through the time series reduction process.

cate that one should expect to see the largest signal at a period equal to $\nu_0/2$, which for standard models of α Cen A is expected to be $\sim 59 \mu\text{Hz}$ (Demarque, Guenther, and van Alstena 1986). No outstanding peaks are seen in this period range. There is a broad peak on the long-period side of the $82 \mu\text{Hz}$ frequency spacing reported by Gelly, Grec, and Fossat

(1986, 1988), but for reasons we shall now discuss, we doubt its significance.

We performed a large number of simulations of our analysis procedure applied to artificial oscillations signals in the presence of noise. In these experiments we synthesized a stellar oscillations signal based on frequencies computed from a

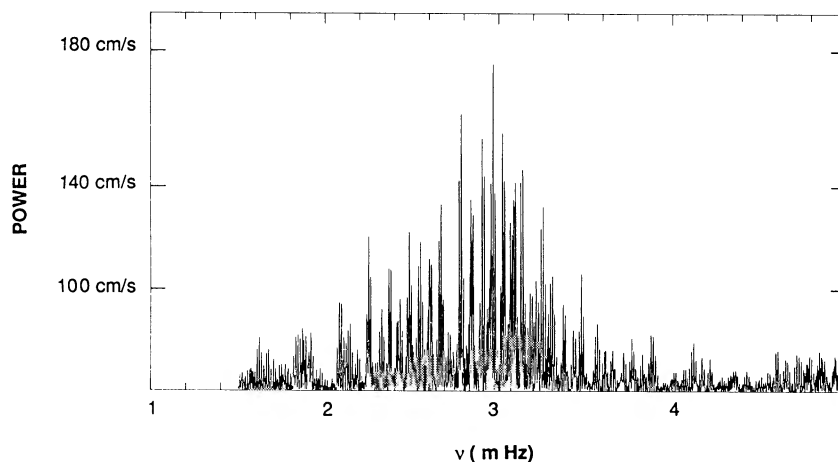


FIG. 3.—Power spectrum of a simulated oscillations data set, using a noise level equal to that in the current observations, and oscillation amplitudes less than or equal to 1.5 ms^{-1} per mode, comparable to those reported by Gelly, Grec, and Fossat (1986). A few peaks in the spectrum have apparent amplitudes greater than 1.5 ms^{-1} , principally because of constructive interference between modes with $l = 0$ and $l = 2$.

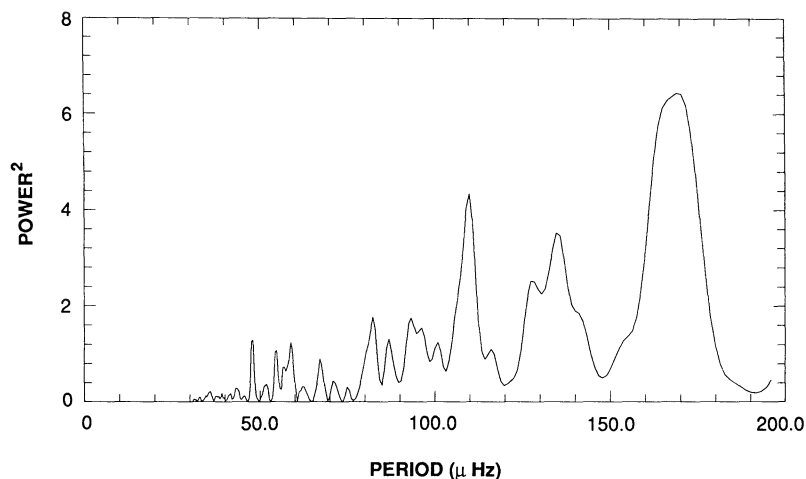


FIG. 4.—Power spectrum of the power spectrum of the Doppler signal shown in Fig. 2a, weighted so that only frequencies between roughly 1.5 and 3.5 mHz contribute to the result. Note that the abscissa is period (in μHz), not the time-like inverse frequency units used by Gelly, Grec, and Fossat (1988).

model of α Cen A, and an amplitude distribution produced by scaling the observed solar amplitude envelope in frequency. The frequency scaling was such as to approximately maintain the ratio between the peak of the amplitude envelope and the acoustic cutoff frequency in the stellar photosphere. The amplitude of each oscillation mode was taken to be that of the amplitude envelope at that frequency, and the phases were taken to be random. Each experiment consisted of adding this oscillating signal, multiplied by an amplitude scale factor, to several realizations of random noise, each with rms equal to that in our observed data. By comparing the results of several realizations conducted with the same input amplitude, we could then estimate how large an input signal is required to produce a robust signature in the power spectrum of the power spectrum.

Based on these simulations, we believe that the peaks seen in the power spectrum of the power spectrum are not significant. In the absence of any signal at all, peaks of amplitude comparable to those seen in Figure 4 appear routinely in the simulations, throughout the interesting band of periods. In order to obtain a clear detection with our noise level and observing intervals, the simulations indicated that oscillation amplitudes near the peak of the amplitude distribution would have to be $\sim 60 \text{ cm s}^{-1}$, or roughly three times the solar amplitude. Even this estimate is perhaps somewhat optimistic, since in a real stellar oscillation signal one would not expect the mode amplitudes to be identically equal to the envelope amplitude. Rather, one expects the amplitudes to be random, with expectation values that follow the amplitude envelope. The resulting irregularity in the power spectrum of the oscillating signal acts to decrease its detectability.

Another approach to determining whether a stellar signal is to be found in the power spectra is to examine the distribution of power values. If one averages together N independent spectra of the same white noise process, then the resulting power estimates at each frequency have a χ^2 distribution with $2N$ degrees of freedom (Groth 1975). If the observed power spectrum (or an average of several spectra) shows a power distribution that is markedly different from the expected one, this is evidence that the input data reflect something other than a simple noise process. A significant stellar oscillations signal, for instance, would be indicated by a significant excess of

points with high power. We used the Kolmogorov-Smirnov test (Press *et al.* 1986, p. 469) to determine whether the differences between the observed distributions and those expected from noise alone are significant.

As estimated by the Kolmogorov-Smirnov test, the probability that the observed power spectrum (Fig. 2a) could be produced by white noise is rather small (~ 0.02). The sense of the difference between the observed and theoretical power distributions is indeed that there is a slight excess of large peaks. It is not clear, however, that this difference arises from a stellar signal. Any slow variation of background noise level with frequency (such as that imposed by high-pass filtering the time series, for example) could produce a similar effect. Also, the corresponding probabilities for spectra of simulated time series with moderate components of oscillating signal tended to be far smaller: less than 10^{-5} , rather than 10^{-2} .

As a final test to decide whether the power spectrum anomalies were related to a stellar signal, we used the complete power spectrum to produce *echelle diagrams*. In an echelle diagram, the one-dimensional spectrum is displayed as a two-dimensional raster image, with a frequency step between raster lines called the *folding frequency*. If the folding frequency is chosen to be ν_0 (or $\nu_0/2$), then modes with successive n values fall along vertical lines in the echelle diagram. Such diagrams have been used with considerable success in the solar case (e.g., Toomre 1986), and have been applied to stellar observations by Gelly, Grec, and Fossat (1986). With the current data set, we found that there are folding frequencies for which the power appears to organize itself into vertical bands, but unfortunately there are several such folding frequencies, and none is particularly outstanding. A statistical test (again based on the Kolmogorov-Smirnov test) of the significance of the preferred folding frequencies again showed no evidence for the presence of solar-like oscillations.

V. CONCLUSIONS

Based on the analysis described above, we believe that p -mode oscillations have not yet been detected in α Cen A. We can set an upper limit on the possible amplitude of $80\text{--}100 \text{ cm s}^{-1}$ (4–5 times solar amplitude) in the Doppler signal, or a few times 10^{-5} (~ 10 times the solar amplitude) in the line depth signal. We think that these are rather firm limits; larger signals

than those indicated almost certainly would have been detected. The astrophysical importance of these limits is probably slight, since there is no obvious reason to expect α Cen A to oscillate with much more than solar amplitude. On the other hand, the Doppler limit is significantly lower than the α Cen A oscillation amplitude reported by Gelly, Grec, and Fossat (1986), suggesting that this previously reported detection is probably erroneous.

These observations, combined with others made with different fiber-fed spectrographs at CTIO and KPNO, have convinced us that most of the noise in this kind of stellar Doppler measurement comes not from photon noise, but from instrumental instabilities that can be controlled. Assuming that methods can be devised to eliminate such instabilities, it should then be possible to measure oscillations in the Doppler signal from other stars, with precision limited by photon statistics. For the instrumental setup used for the current work (1.5 m telescope, 30 nm spectral coverage at a resolution of 34,000, total system transmission $\sim 1\%$), this limit is $\sim 1.5 \text{ m s}^{-1}$ for a

60 s integration on α Cen A (a G dwarf of magnitude 0.2). These values may be compared with those derived by Connes (1985) for the performance of an optical stellar accelerometer. Allowing for the differences in assumed spectrograph wavelength coverage, transmission, and resolution, the noise figures agree quite well. After dealing with spectrograph instability, the next challenge in Doppler asteroseismology will therefore be in spectrograph design. Substantial increases in spectral resolution are not necessary, but measuring fainter stars with adequately low noise will require major improvements in both transmission and bandpass.

We are grateful to Tom Ingerson and the staff of CTIO for their excellent support in obtaining the observations and in understanding the spectrograph system. We also thank Rose Reynolds for her assistance with aspects of the data reduction, and Drake Deming for his careful reading of an early version of this paper.

REFERENCES

- Brown, T. M., and Morrow, C. A. 1987, *Ap. J. (Letters)*, **314**, L21.
 Connes, P. 1985, *Ap. Space Sci.*, **110**, 211.
 Christensen-Dalsgaard, J. 1988, in *Advances in Helio- and Asteroseismology*, ed. J. Christensen-Dalsgaard and S. Frandsen (Dordrecht: Reidel), p. 295.
 Demarque, P., Guenther, D. B., and van Altena, W. F. 1986, *Ap. J.*, **300**, 773.
 Flannery, B. P., and Ayres, T. R. 1978, *Ap. J.*, **221**, 175.
 Frandsen, S. 1984, in *Theoretical Problems in Stellar Stability and Oscillations* (Proc. 25th Liege Colloquium, University de Liege), p. 303.
 Gelly, B., Grec, G., and Fossat, E., 1986, *Astr. Ap.*, **164**, 383.
 ———. 1988, in *Advances in Helio- and Asteroseismology*, ed. J. Christensen-Dalsgaard and S. Frandsen (Dordrecht: Reidel), p. 249.
 Gilliland, R. L., and Brown, T. M. 1988, *Pub. A.S.P.*, **100**, 754.
 Gilliland, R. L., and Däppen, W. 1988, *Ap. J.*, **324**, 1153.
 Gough, D. O. 1987, *Nature*, **326**, 257.
 Groth, E. J. 1975, *Ap. J. Suppl.*, **29**, 286.
 Harvey, J. W. 1988, in *Advances in Helio- and Asteroseismology*, ed. J. Christensen-Dalsgaard and S. Frandsen (Dordrecht: Reidel), p. 497.
 Holweger, H., and Testerman, L. 1975, *Solar Phys.*, **43**, 271.
 Horne, K. 1986, *Pub. A.S.P.*, **98**, 609.
 Noyes, R. W., Baliunas, S. L., Belserene, E., Duncan, D. K., Horne, J., and Widrow, L. 1984, *Ap. J.*, **285**, L23.
 Press, W. H., Flannery, B. P., Teukolsky, S. A., and Vetterling, W. T. 1986, *Numerical Recipes: The Art of Scientific Computing* (Cambridge: Cambridge University Press).
 Toomre, J. 1986, in *Seismology of the Sun and the Distant Stars*, ed. D. O. Gough (Dordrecht: Reidel), p. 1.

TIMOTHY M. BROWN: High Altitude Observatory, P.O. Box 3000, Boulder, CO 80307

RONALD L. GILLILAND: Space Telescope Science Institute, Homewood Campus, Johns Hopkins University, Baltimore, MD 21218